www.czasopisma.pan.pl PAN POLSKA AKADEMIA NAUK www.journals.pan.pl

A R C H I V E S O F M E T A L L U R G Y A N D M A T E R I A L S

Volume 56 2011 Issue 2

DOI: 10.2478/v10172-011-0037-5

A. KULAWIK* A. BOKOTA*

MODELLING OF HEAT TREATMENT OF STEEL ELEMENTS WITH THE MOVEMENT OF COOLANT

MODELOWANIE OBRÓBKI CIEPLNEJ ELEMENTÓW STALOWYCH Z UWZGLĘDNIENIEM RUCHÓW CHŁODZIWA

A mathematical and numerical model of hardening process using the generalized finite difference method for the movement of fluid and heat transport have been proposed in this paper. To solve the Navier-Stokes equation the characteristic based split scheme (CBS) has been used. The solution of the heat transport equation with the convective term has been obtained by a stabilized meshless method. To determine of the phase transformation the macroscopic model built on the basis of CCT diagrams for continuous cooling of medium-carbon steel has been used. The temporary temperature fields, the phase transformation, thermal and structural strains for the heat treated element and the fields of temperature and velocity for the coolant have been determined. The comparative analysis of the results of calculations for the model without taking into account movement of coolant has been carried out. The effect of the notch in the shaft on the cooling rates and fields of the kinetics of the phase transformations has been presented.

Keywords: heat treatment, continuous cooling, meshless method, liquid coolant

W pracy zaproponowano model matematyczny i numeryczny zjawisk termicznych oraz ruchów chłodziwa zbudowany z wykorzystaniem uogólnionej metody różnic skończonych. Do rozwiązania równania Naviera-Stokesa wykorzystano metodę rzutowania (CBS). Rozwiązanie równania przewodzenia ciepła z członem konwekcyjnym uzyskano na podstawie stabilizowanej bezsiatkowej metody różnic skończonych. Do modelowania przemian fazowych wykorzystano makroskopowy model zbudowany na podstawie analizy wykresów ciągłego chłodzenia CTPc dla stali średniowęglowej. Dla elementu obrabianego cieplnie określono chwilowe pola temperatury, udziały fazowe, odkształcenia termiczne, strukturalne oraz pala temperatury i prędkości cieczy chłodzącej. Przeprowadzono analizę porównawczą z wynikami obliczeń z ruchem i bez ruchu chłodziwa. W pracy przedstawiono także wpływ wycięcia (rowka na wałku) na pola prędkości chłodziwa oraz na kinetykę przemian fazowych.

1. Introduction

The process of heat treatment of steel elements is a complex and difficult phenomenon to numerical modelling. There are many factors which have a significant impact on the processes of quenching and tempering, such as process conditions, properties of the workpiece, or the properties of the coolant [1,2]. A multitude of these parameters leads researchers interested in modelling of hardening to continuing extend the scope of considered of phenomena of such a process. Generally, in the models of the hardening process the influence of convective cooling fluid movements is not taken into account. On the whole, the impact of coolant on the temperature of element is modeled by suitable boundary conditions, which are oversimplifying the modelling, but do not take into consideration the influence of large temperature gradients on the edges of the cooling element and generating strong convective motion of the coolant [3,4]. In the paper, the effect of convection movements of quenching coolant on the structure and stresses of component after heat treatment has been analyzed.

* CZESTOCHOWA UNIVERSITY OF TECHNOLOGY, INSTITUTE OF COMPUTER AND INFORMATION SCIENCES, 42-200 CZĘSTOCHOWA, 73 DĄBROWSKI STR., POLAND

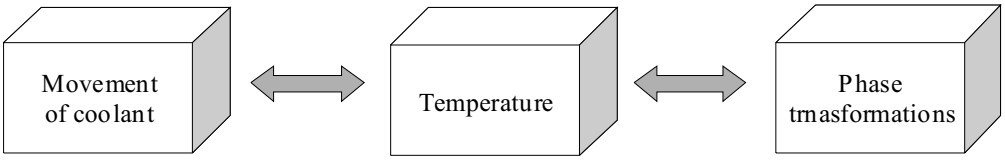

Fig. 1. Conceptual diagram of the analyzed problem

2. Temperature fields

In modelling the processes of heat treatment have a significant role taken into account movements of natural or a forced convection. These movements usually occurring in the coolant are approximated by the appropriate boundary conditions. However, this approach may lead to a large error of approximation. This occurs when the coolant is liquid, and also for geometrically complex parts of machines. Therefore, the model of heat transport for heat treatment processes should take into account the movements of the liquid coolant. In presented paper a numerical model of heat transfer for the coolant and the cooled axisymmetric element in the hardening process is described.

The temperature fields are determined on the basis of the heat transfer equation with convection term, which for axially symmetric space take the following form:

$$\frac{\lambda}{r}\frac{\partial T}{\partial r}+\frac{\partial}{\partial r}\left(\lambda\frac{\partial T}{\partial r}\right)+\frac{\partial}{\partial z}\left(\lambda\frac{\partial T}{\partial z}\right)- -\rho C\left(V_r\frac{\partial T}{\partial r}+V_z\frac{\partial T}{\partial z}\right)-\rho C\frac{\partial T}{\partial t}=q_V \tag{1}$$

where T [K] is the temperature, t [s] is the time, $\lambda = \lambda(T)$ [W/mK] is the thermal conductivity, ρ [kg/m^3] is the density, C [J/kgK] is the specific heat, V [m/s] is the velocity, q_v [J/m^{3}s] is the volumetric heat source, r – is a distance from the symmetry axis.

In equation (1) latent heat of the phase transformation as volumetric heat source in heat transfer equation is introduced:

$$q_V=\sum_i H_i\frac{\Delta\eta_i}{\Delta t}\rho \tag{2}$$

where: $H_i[J/kg]$ is the heat of the "i" transformation, $\Delta\eta_i$ is the volumetric increment of the "i" phase.

For high- and medium-carbon steel should be taken into account changes in temperature caused by latent heats of the phase transformation. The effect of these reactions is significant on the cooling temperature. This is particularly visible during the hardening process when a high volume transformation austenite to pearlite occurs. In the literature of latent heat of phase transformation the models, heat of transformation for particular phase (dependent on the temperature and chemical composition) are described [2]. In presented paper the results of analysis of Fe-C-Mn system and constant value of enthalpy for austenite-martensite transformation are used [2,5]. This solution is approximated by the polynomial function of the third degree:

$$\begin{aligned} H_{\gamma\to\alpha}(T) &= 0.00064156\cdot T^3-0.59347\cdot T^2+ \\ &\quad +245.24\cdot T-145423 \\ H_{\gamma\to P}(T) &= 0.00093038\cdot T^3-1.0536\cdot T^2+ \\ &\quad +475.96\cdot T-212728 \\ H_{\gamma\to B}(T) &= 0.00077541\cdot T^3-0.81671\cdot T^2+ \\ &\quad +365.01\cdot T-176705 \\ H_{\gamma\to M}(T) &= 8.25\cdot 10^4 \end{aligned} \tag{3}$$

where: $H_{\gamma\to\alpha}$[J/kg] is the heat of austenite to ferrite transformation, $H_{\gamma\to P}$ is the heat of austenite to pearlite transformation, $H_{\gamma\to B}$ is the heat of austenite to bainite transformation, $H_{\gamma\to M}$ is the heat of austenite to martensite transformation, T is the temperature [°C].

As already indicated, the latent heats of the transformations have especially influence on the changes of temperature and on the kinetics of the phase transformations in the volumetric hardening for high or medium carbon steels, whereas it is insignificant in the transformations during the surface hardening for these steels.

2.1. Numerical method

Modelling of technological processes is a difficult task and sets many problems for developer. Incorporation of the characteristic features of the phenomena occurring in the modeled process is fundamental into any correctness model. Selection of method at the beginning construction of application is very significant. Potential problems in modelling often occur as a result of the wrong choice modelling method, therefore it is important to know the advantages and disadvantages of the chosen method of modelling. Unfortunately, on the beginning of development of a model is rarely possible predicted the future problems and pathways of algorithm development. Because of its advantages the generalized finite difference method has been chosen. This choice is related to, inter alia, easy adaptation to the changes of mesh geometry.

For the modelling of heat flow the generalized finite difference method was used [6,7]. So that a function of

temperature has been developed into Taylor series with an accuracy to the second derivative:

$$T_j = T_i + \left(\frac{\partial T}{\partial r}\right)_i h_j + \left(\frac{\partial T}{\partial z}\right)_i k_j + \frac{1}{2}\left(\frac{\partial^2 T}{\partial r^2}\right)_i h_j^2 + \\ + \frac{1}{2}\left(\frac{\partial^2 T}{\partial z^2}\right)_i k_j^2 + \left(\frac{\partial^2 T}{\partial r \partial z}\right)_i h_j k_j \tag{4}$$

where: $h_j = r_j - r_i$, $k_j = z_j - z_i$, "i" number of the central-node, "j" additional numbers of nodes around the central node.

The following criterion for the quality of approximations derived in the central node has been assumed:

$$J = \sum_{j=1}^{n} \left(\left(T_i - T_j + \left(\frac{\partial T}{\partial r}\right)_i h_j + \left(\frac{\partial T}{\partial z}\right)_i k_j + \frac{1}{2}\left(\frac{\partial^2 T}{\partial r^2}\right)_i h_j^2 + \right.\right. \\ \left.\left. + \frac{1}{2}\left(\frac{\partial^2 T}{\partial z^2}\right)_i k_j^2 + \left(\frac{\partial^2 T}{\partial r \partial z}\right)_i h_j k_j \right) \frac{1}{l_j^m} \right)^2 \tag{5}$$

where: l_j is the distance from the "j" node to central node ("i"), a constant m=3.

The necessary conditions for a minimum of functional J are zeroing to derivatives:

$$\frac{\partial J}{\partial (T,_\alpha)_i} = 0, \quad \frac{\partial J}{\partial \left(T,_{\alpha\beta}\right)_i} = 0 \tag{6}$$

where $T,_\alpha = \partial(.)/\partial x_\alpha$.

Finally, the solution of equations (6) are the coefficients z_j, used to build the matrix in the selected numerical method.

2.2. Stabilization method

Numerical modelling of the phenomena with high rates causes the problems with the stabilization of solutions. Therefore, the stabilization of the differential method using a combination of derivatives (determined on

The modification of the coefficients in the stabilization of generalized finite difference method, GFDM is described by the following equation:

$$z_\alpha = (1 - \zeta_\alpha) z_\alpha^I + \zeta_\alpha z_\alpha^j, \quad j = \text{II} \; .. \; \text{V}, \\ \zeta_\alpha = \frac{1}{2}\left| \frac{1}{\tanh(Pe_\alpha/2)} - \frac{2}{Pe_\alpha} \right| \tag{7}$$

where Pe is a local *Peclet* number defined as follows: in the heat transfer model - $Pe_\alpha = v_\alpha r_\alpha \rho C/\lambda$, in the flow model - $Pe_\alpha = \rho v_\alpha r_\alpha/\mu$, r_α is a characteristic size of the element of grid in the α direction, j is the number of grid (see Fig. 2). several nodal grids of nodes) was proposed.

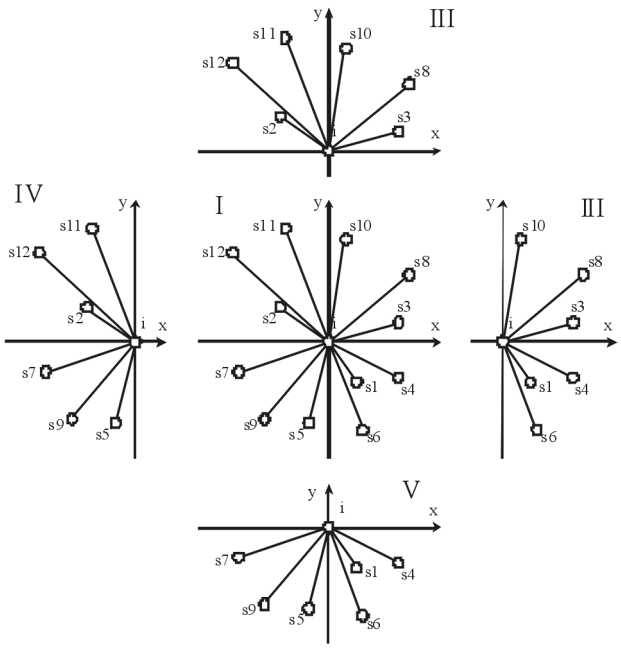

Fig. 2. Examples of grid nodes used for the calculation

2.3. Numerical model

The temperature in nodes was determined by the solution of the heat transfer equation with the convective term based on GFDM. This solution in a nonlinear implicit time scheme is written in the matrix form as:

$$\mathbf{A} \cdot \mathbf{T} = \mathbf{D} \tag{8}$$

where matrix **A** is defined as:

$$A_{i,i} = \lambda \left(- \sum_{j=1}^{n} \left(z_j^{xx} + z_j^{yy} \right) - \frac{1}{r_i} \sum_{j=1}^{n} \left(z_j^x \right) \right) + \\ + \rho C \left(\sum_{j=1}^{n} z_j^x (V_x)_i + \sum_{j=1}^{n} z_j^y \left(V_y \right)_i \right) \\ A_{i,j} = \lambda \left(z_j^{xx} + z_j^{yy} \right) + \frac{\lambda}{r_i} z_j^x - \rho C \left(z_j^x (V_x)_i + z_j^y \left(V_y \right)_i \right) \tag{9}$$

and vector **D** is written as:

$$D_i = -\frac{\rho C}{\Delta t} T_i^{s-1} - q_i^V - \\ - \frac{\Delta \lambda}{\Delta T} \left(\sum_{j=1}^{n} z_j^x T_j^{s-1} - \sum_{j=1}^{n} z_j^x T_i^{s-1} + \sum_{j=1}^{n} z_j^y T_j^{s-1} - \sum_{j=1}^{n} z_j^y T_i^{s-1} \right) \tag{10}$$

where $z_j^\alpha, z_j^{\alpha\alpha}$ are the coefficients determined from the solutions of the equation (6), s is the number of the time step, i and j are the numbers of central and surrounding nodes of the grid nodes (see Fig. 2).

Because the presented system matrix is highly asymmetric, it was solved by using the biconjugated gradients method. In this iterative method was used the Jacobi preconditioner [8,9].

3. Velocity fields

In modelling of the hardening process, especially when the coolant is a liquid, should be considered the behavior of the cooling medium. In this process the large changes in the intensity occurring in cooling were caused by convection or forced movement of liquid. The basis for the mathematical description of this movement is the Navier-Stokes equation with the free convection term.

The Navier-Stokes equation is defined as follows [10,11]:

$$\begin{aligned}
&\mu\left(\frac{\partial^2 V_r}{\partial r^2}+\frac{1}{r}\frac{\partial V_r}{\partial r}+\frac{\partial^2 V_r}{\partial z^2}-\frac{V_r}{r^2}\right)-\frac{\partial p}{\partial r}= \\
&=\rho\left(\frac{dV_r}{dt}+V_r\frac{\partial V_r}{\partial r}+V_z\frac{\partial V_r}{\partial z}\right) \\
&\mu\left(\frac{\partial^2 V_z}{\partial r^2}+\frac{1}{r}\frac{\partial V_z}{\partial r}+\frac{\partial^2 V_z}{\partial z^2}\right)-\frac{\partial p}{\partial z}+\rho a_z\beta\left(T-T_{ref}\right)= \\
&=\rho\left(\frac{dV_z}{dt}+V_r\frac{\partial V_z}{\partial r}+V_z\frac{\partial V_z}{\partial z}\right)
\end{aligned} \tag{11}$$

where V[m/s] is the velocity component in the r or z-direction, μ [kg/ms] is the dynamic viscosity, p [N/m^2] is the pressure, a_z [m/s^2] is the acceleration component in the z-direction, β [1/K] is the volumetric thermal expansion coefficient, T_{ref} [K] is the reference temperature.

The Navier-Stokes equation (11) is supplemented by the continuity equation taking the form:

$$\frac{\partial V_r}{\partial r}+\frac{V_r}{r}+\frac{\partial V_z}{\partial z}=0 \tag{12}$$

Equations (11) and (12) are complemented by appropriate boundary and initial conditions.

The Navier-Stokes equation (11) is solved only in a region filled with the coolant by means of a characteristic based split (CBS) scheme. The CBS scheme is based on the projection method developed by Chorin [12] and described by Zienkiewicz and Codina [10]. In this method an auxiliary velocity field $V*$ is introduced to uncouple equations (11) and (12).

$$\begin{aligned}
&\frac{V_r^*-V_r^k}{\Delta t}=\frac{\mu}{\rho}\left(\frac{\partial^2 V_r}{\partial r^2}+\frac{1}{r}\frac{\partial V_r}{\partial r}+\frac{\partial^2 V_r}{\partial z^2}-\frac{V_r}{r^2}\right)- \\
&-\left(V_r\frac{\partial V_r}{\partial r}+V_z\frac{\partial V_r}{\partial z}\right) \\
&\frac{V_z^*-V_z^k}{\Delta t}=\frac{\mu}{\rho}\left(\frac{\partial^2 V_z}{\partial r^2}+\frac{1}{r}\frac{\partial V_z}{\partial r}+\frac{\partial^2 V_z}{\partial z^2}\right)+ \\
&+a_z\beta\left(T-T_{ref}\right)-\left(V_r\frac{\partial V_z}{\partial r}+V_z\frac{\partial V_z}{\partial z}\right)
\end{aligned} \tag{13}$$

where V_α^k is the velocity component in the r or z-direction for the previous time step.

The final velocity field is corrected by the pressure increment so that is divergence free:

$$V_\alpha-V_\alpha^*=-\frac{\Delta t}{\rho}p_{,\alpha} \tag{14}$$

By taking the divergence of (14) the following Poisson equation for the pressure is obtained:

$$\frac{\Delta t}{\rho}\left(\frac{\partial^2 p}{\partial r^2}+\frac{1}{r}\frac{\partial p}{\partial r}+\frac{\partial^2 p}{\partial z^2}\right)=\frac{\partial V_r^*}{\partial r}+\frac{V_r^*}{r}+\frac{\partial V_z^*}{\partial z} \tag{15}$$

The final velocity field is corrected by the pressure increment:

$$V_\alpha=V_\alpha^*+\Delta V_\alpha^*,\ \Delta V_\alpha^*=-\frac{\Delta t}{\rho}\left(p_{,\alpha}\right) \tag{16}$$

The momentum equation (13) was solved by GDFM using an implicit time scheme for i-th node of the grid. This solution in the matrix form is written as:

$$\mathbf{A}^\alpha\cdot\mathbf{V}^{\alpha*}=\mathbf{D}^\alpha \tag{17}$$

where matrix $\boldsymbol{A}^\alpha$ is described as:

$$\begin{aligned}
A_{i,i}^x&=1-\Delta t\left(\frac{\mu}{\rho}\left(-\frac{1}{r_i^2}-\sum_{j=1}^{n}\left(z_j^{xx}+z_j^{yy}\right)+\frac{1}{r_i}\sum_{j=1}^{n}z_j^x\right)\right) \\
A_{i,i}^y&=1-\Delta t\left(\frac{\mu}{\rho}\left(-\sum_{j=1}^{n}\left(z_j^{xx}+z_j^{yy}\right)+\frac{1}{r_i}\sum_{j=1}^{n}z_j^x\right)\right) \\
A_{i,j}^\alpha&=\frac{\Delta t\mu}{\rho}\left(-\left(z_j^{xx}+z_j^{yy}\right)-\frac{1}{r_i}z_j^x\right)
\end{aligned} \tag{18}$$

and vector $\boldsymbol{D}^\alpha$ is written as:

$$\begin{aligned}
D_i^\alpha&=\left(V_\alpha^{s-1}\right)_i- \\
&-\Delta t\left(a_\alpha\beta\left(T_i-T_\infty\right)+\left(\sum_{j=1}^{n}z_j^{(\gamma)}V_{\alpha j}^{s-1}-\sum_{j=1}^{n}z_j^{(\gamma)}V_{\alpha i}^{s-1}\right)\right)
\end{aligned} \tag{19}$$

The pressure field is obtained by solving the Poisson equation (15), which in the matrix form is written as:

$$\mathbf{A}\cdot\mathbf{p}=\mathbf{D} \tag{20}$$

where matrix $\boldsymbol{A}$ is described as:

$$\begin{aligned}
A_{i,i}&=\frac{1}{\rho}\left(-\sum_{j=1}^{n}\left(z_j^{xx}+z_j^{yy}\right)-\frac{1}{r_i}\sum_{j=1}^{n}\left(z_j^x\right)\right) \\
A_{i,j}&=\frac{1}{\rho}\left(z_j^{xx}+z_j^{yy}+\frac{z_j^x}{r_i}\right)
\end{aligned} \tag{21}$$

and vector $\boldsymbol{D}$ is written as:

$$\begin{aligned}
D_i=\frac{1}{\Delta t}&\left(\sum_{j=1}^{n}z_j^x\left(V_x^*\right)_j-\sum_{j=1}^{n}z_j^x\left(V_x^*\right)_i+\sum_{j=1}^{n}z_j^y\left(V_y^*\right)_j-\right. \\
&\left.-\sum_{j=1}^{n}z_j^y\left(V_y^*\right)_i+\frac{\left(V_x\right)_i}{r_i}\right)
\end{aligned} \tag{22}$$

However, the equation (16) in the generalized finite difference method has in the form:

$$\Delta V_{\alpha i}^*=-\frac{\Delta t}{\rho}\left(\sum_{j=1}^{n}z_j^{(\alpha)}p_{\alpha j}-\sum_{j=1}^{n}z_j^{(\alpha)}p_{\alpha i}\right) \tag{23}$$

4. Phase transformations of cooling

The modelling of thermal phenomena, except movements of the liquid coolant, should also take into consideration the phase transformations in the solid state. These transformations influence on the temperature field through the heat of transformation and also have a significant impact on the temporary and residual field of stresses. In the paper the macroscopic model of the phase transformations based on an analysis of CCT diagrams has been presented [4,13].

The volume fractions $\eta_{(.)}(T,t)$ growth during cooling process are calculated by the Avrami equations [13,14].

$$\eta_{(i)}(T,t) = \min\left\{\eta_{(i\%)}, \tilde{\eta}_\gamma - \sum_{j\neq i}\eta_j\right\}\cdot\left(1-\exp\left(-b(T)\,t^{n(T)}\right)\right) \tag{24}$$

where: $\tilde{\eta}_\gamma$ is a volume fraction of forming austenite, η_j is volume fraction of phase formed during cooling process, $\eta_{(i\%)}$ is final fraction of "i"-phase estimation of basis on CCT diagrams considered steel. The functions $b(T)$ and $n(T)$ depending on temperature as well as on the start (t_s) and finish (t_f) times of transformation is described by formulas:

$$n(T) = 6,12733/\ln\left(\frac{t_f(T)}{t_s(T)}\right), \qquad b(T) = \frac{0,01005}{t_s^{n(T)}} \tag{25}$$

The results obtained from Avrami equation strongly depend on the assumed CCT diagram analysis. The function determined by the Avrami covers the whole range transformation and must be appropriately modified for the analysis of individual transformation. Is assumes that the function is defined in segments depending on the location of the transformation in the CCT diagram. Coefficients occurring in these functions are obtained from CCT diagram. In presented model kinetics of the phase transformation are determined by the Avrami equations. Three variants of phase kinetics are considered according to informations about creation of particular phase. In paper the model, which determinate the kinetics of individual phases with the use of spline functions is applied. If maximum value of participation of the particular phase and final time of its creation is predicted, the beginning of the phase transformation will be calculated from following equation [4,13]:

$$t_s\left(t,\eta_\%,t_f\right) = \left(\frac{t^{\frac{A}{B(\eta_\%)}}}{t_f}\right)^{\left(\frac{B(\eta_\%)}{A-B(\eta_\%)}\right)} \tag{26}$$

where: $\eta_\%$ is estimated volume fraction of the last phase.

If the end of first transformation, its maximum participation and starting time of the transformations is known, ending of the transformations will be estimated from below relation [13]:

$$t_f(t,\eta_\%,t_s) = \exp\left(\frac{-A\cdot(\ln(t_s)-\ln(t))}{B(\eta_\%)}\right)\cdot t_s \tag{27}$$

In the case of the phase transformation occurring between others transformations, the start of them is calculated from following equation [13]:

$$t_s(t_1,\eta_{(1\%)},t_2,\eta_{(2\%)}) = \\ = \sqrt{\left(\frac{t_1^{\frac{B(\eta_{(1\%)})}{A}}}{\exp\left(-\frac{A}{B(\eta_{(2\%)})}\cdot\ln(t_2)\right)}\right)^{\frac{B(\eta_{(1\%)})}{A-B(\eta_{(1\%)})}}}^{N(\eta_{(1\%)},\eta_{(2\%)})} \tag{28}$$

The coefficients A(), B(), and N() are calculated using following formulas:

$$N(\eta_{(1\%)},\eta_{(2\%)}) = \left(\frac{-A}{B(\eta_{(2\%)})}+1\right)\left(\frac{B(\eta_{(1\%)})}{A-B(\eta_{(1\%)})}\right)+1 \tag{29}$$

$$A = \exp\left(\ln\left(\frac{\ln\left(1-\eta_f^i\right)}{\ln\left(1-\eta_s^i\right)}\right)\right), \qquad B(\eta_\%) = \ln\left(\frac{\ln(1-\eta_\%)}{\ln(1-\eta_s)}\right) \tag{30}$$

Among considerable factors deciding in primary measure about course of transformation are stress conditions. In this model modification of equations describing kinetics of the phase transformations are introduced [3,15,16]. Influence of the mechanical phenomena on the changes of material microstructure is taken into account. This phenomenon is especially noticeable during the martensite transformation. This effect describes as dependence of start martensite temperature on average and effective stresses.

The phase transformation during the high-rate cooling (transformation austenite to martensite) is determined by classic form of Koistinen-Marburger equation [3,15-17]:

$$\eta_M(T,t) = \left(\tilde{\eta}_\gamma - \sum_{i\neq M}\eta_i\right) \\ \left(1-\exp\left(-k\left(M_S - T + A_M\sigma_{eff} + B_M\sigma_a\right)\right)\right),\ k = 0.01537 \tag{31}$$

where: $\sigma_a = (\sigma_{ii})/3$ – average stress, $\sigma_{eff} = \sqrt{3/2\,(\sigma^D\cdot\sigma^D)}$ – effective stress, σ^D – deviatoric stresses, A_M and B_M coefficients for C45 steel are equal to $A_M = 1.25\times10^{-6}$ [K/Pa], $B_M = 0.75\times10^{-6}$ [K/Pa] [15].

According to eq. 4.31 it can be noticed, that temperature M_S diminishes when average stress is less than zero, otherwise M_S rises. Effective stress always cause

the growth M_S temperature, so the austenite – martensite transformation is accelerated.

The increase of isotropic strain resulted from the temperature and phase transformation ($d\varepsilon^{Tph} = d\varepsilon^{T} + d\varepsilon^{ph}$) during heating and cooling is described by formula [4,13]:

$$d\varepsilon^{T} = \sum_{i} \alpha_i(T)\,\eta_i dT, \quad d\varepsilon^{ph} = \sum_{i} \varepsilon_i^{ph}(T)\,d\eta_i \tag{32}$$

where: α_i is a thermal expansion coefficients for "i" phase, $\varepsilon_i^{ph} = \delta V_i/(3V)$ is a strain expansion coefficients for "i" transformation. Experimental research and numerical simulations – dilatometric curves, assign these values (thermal and structural expansion coefficients) [13].

The kinetics of the phase transformations during cooling strongly depend on austenisation temperature, therefore model, which exploits two CCT diagrams for C45 steel (880°C and 1050°C austenisation temperature) was developed [18,19]. The constructed application uses a pairs of corresponding points of both CCT diagrams. Each of the points located at the curve determining the end of transformation must have the maximum value of transformation.

Continuous cooling transformation diagrams displaced with respect to each other are used to determine intermediate diagram using follows approximation [13].

$$\begin{aligned} t_j(T_{Aust}) &= \gamma_{Aust} t_j^{1050} + (1-\gamma_{Aust})\, t_j^{880} \\ T_j(T_{Aust}) &= \gamma_{Aust} T_j^{1050} + (1-\gamma_{Aust})\, T_j^{880} \\ \eta_{(i\%)j}(T_{Aust}) &= \gamma_{Aust} \eta_{(i\%)j}^{1050} + (1-\gamma_{Aust})\, \eta_{(i\%)j}^{880} \end{aligned} \tag{33}$$

Parameter γ_{Aust} is described by formula:

$$\begin{aligned} \gamma_{Aust} &= 0 && \text{for} \quad T_{\max} < 880^{\circ}C \\ \gamma_{Aust} &= \tfrac{T_{\max}-880}{1050-880} && \text{for} \quad 880^{\circ}C < T_{\max} < 1050^{\circ}C \\ \gamma_{Aust} &= 1 && \text{for} \quad T_{\max} > 1050^{\circ}C \end{aligned} \tag{34}$$

The presented numerical model for numerical simulations of structural and thermal strains during the phase transformation of cooling for different austenization temperature is used.

5. Evaluations of the models

Numerical models are only a closer reality. Developed mathematical models contain some simplifications influencing on the accuracy of the solution. Therefore, a comparative analysis between calculated and reference results (experimental results and numerical benchmarks) is presented.

The differential equation of heat transport using a generalized finite difference method in the control area Ω was solved. The rectangular geometry of dimensions 1.0×1.0 [m], the initial and boundary conditions were adopted in such a way, that numerical calculations results of the approximate solution can be compared to an existing analytical solution.

As an initial condition we assumed, that the entire area $T_0(x_\alpha)$=300 [K] and the boundary conditions were follows:

- on the left boundary (Γ, x =0) the Dirichlet condition $T_D(x=0)$=1000 [K]
- on the other edge the Neumann condition $q = -\lambda\frac{\partial T}{\partial n} = 0$ [W/m^2]

For this case, the analytical solution has the following form [20]:

$$\begin{aligned} T(x,t) = \tfrac{1}{2}\left(T^D - T_0\right)\left(erfc\left(\tfrac{x-ut}{\sqrt{4Dt}}\right) + \right. \\ \left. + \exp\left(\tfrac{ux}{D}\right) erfc\left(\tfrac{x+ut}{\sqrt{4Dt}}\right)\right) + T_0 \end{aligned} \tag{35}$$

where $D=\lambda/(\rho C)$.

The obtained results are shown in Figure 3.

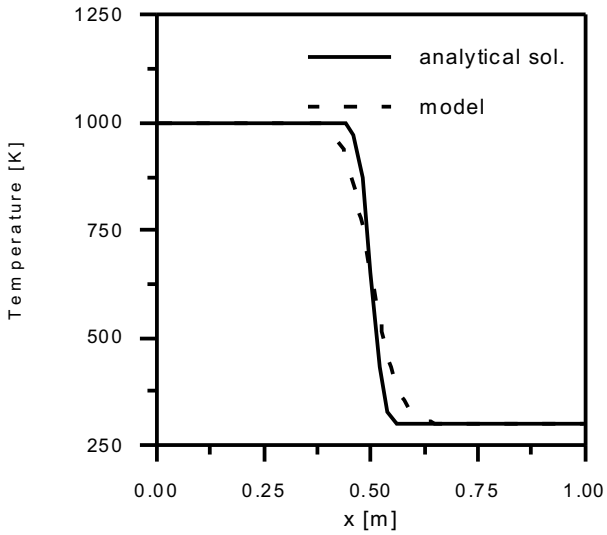

Fig. 3. The comparison of numerical model with the analytical solution, u=1 [m/s], t=0.5 [s], λ=0.5 [W/mK], ρ=1 [kg/m^3], C=1000 [J/kgK]

The numerical model of coolant flow was verified using the numerical benchmarks involving a forced flow in a closed area with a movable top wall (Fig. 4) – Driven Cavity Test (Ghia et al.) [21]. The conditions of the test were as follows: area dimension d=1 [m], density ρ=1 [kg/m^3], dynamic viscosity μ [kg/ms].

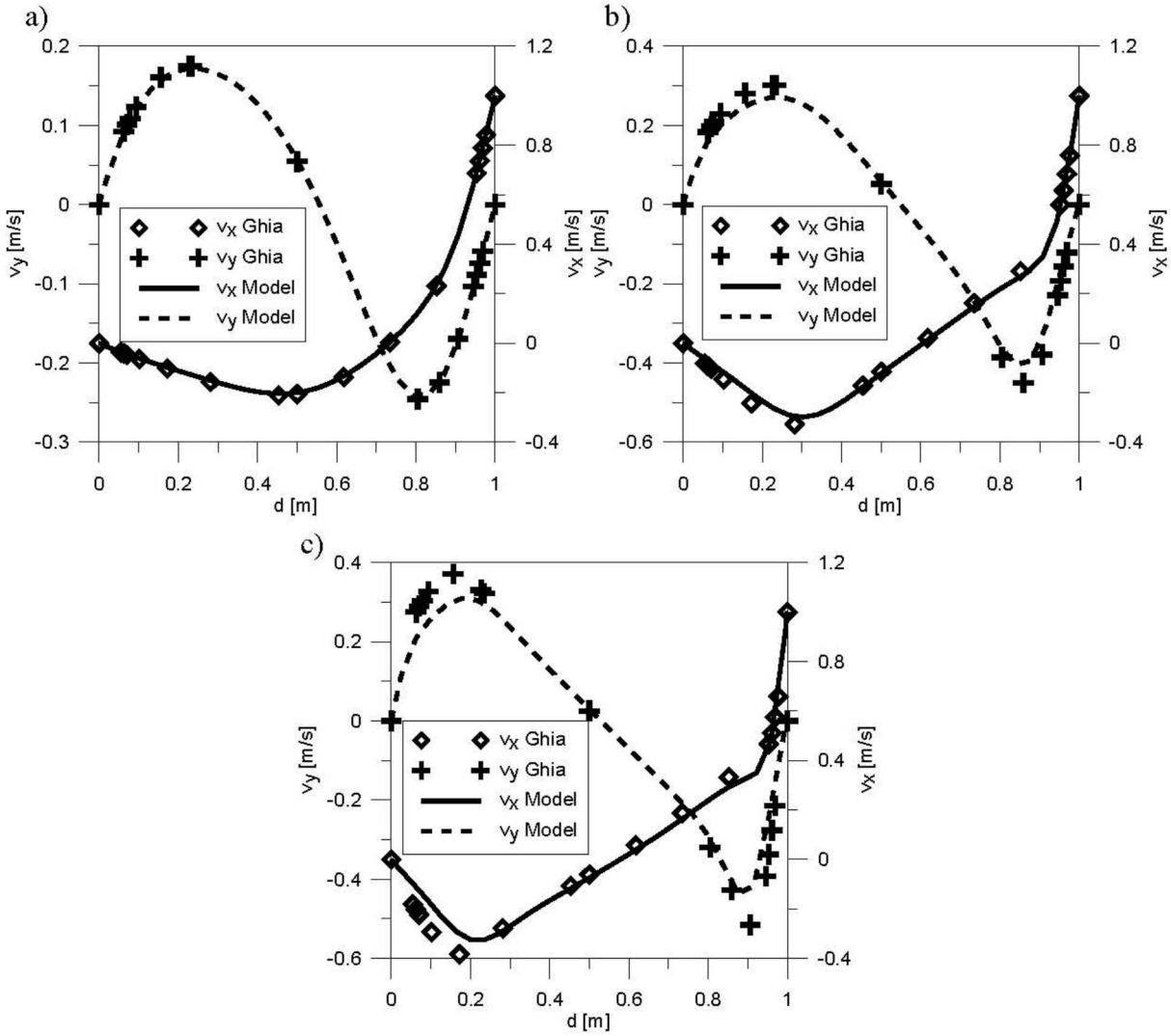

Fig. 4. The comparison of calculation results with the numerical benchmark for the grid 150×150 nodes, a) *Re*=100, b) *Re*=400, c) *Re*=1000

The experimental research to validate the method used to determine the kinetics of the phase transformations during cooling was made. The objects of research were specimens made from C45 steel. The experimental research was done on thermal cycle simulators: SMITWELD TCS 1405, which is the property of Institute of Mechanics and Machine Design of Technical University of Częstochowa. Heating in the dilatometer is realized by the inductive method, while the cooling is executed by water inside the specimen. The dimensions of specimens were 11×11×55 [mm]. In the experimental research the phase transformations during the cooling of continuous steel C45 exposed to quick heating and cooling with different rates (heating – 100 [°C/s], cooling – 10, 30, 200 [°C/s]) were investigated.

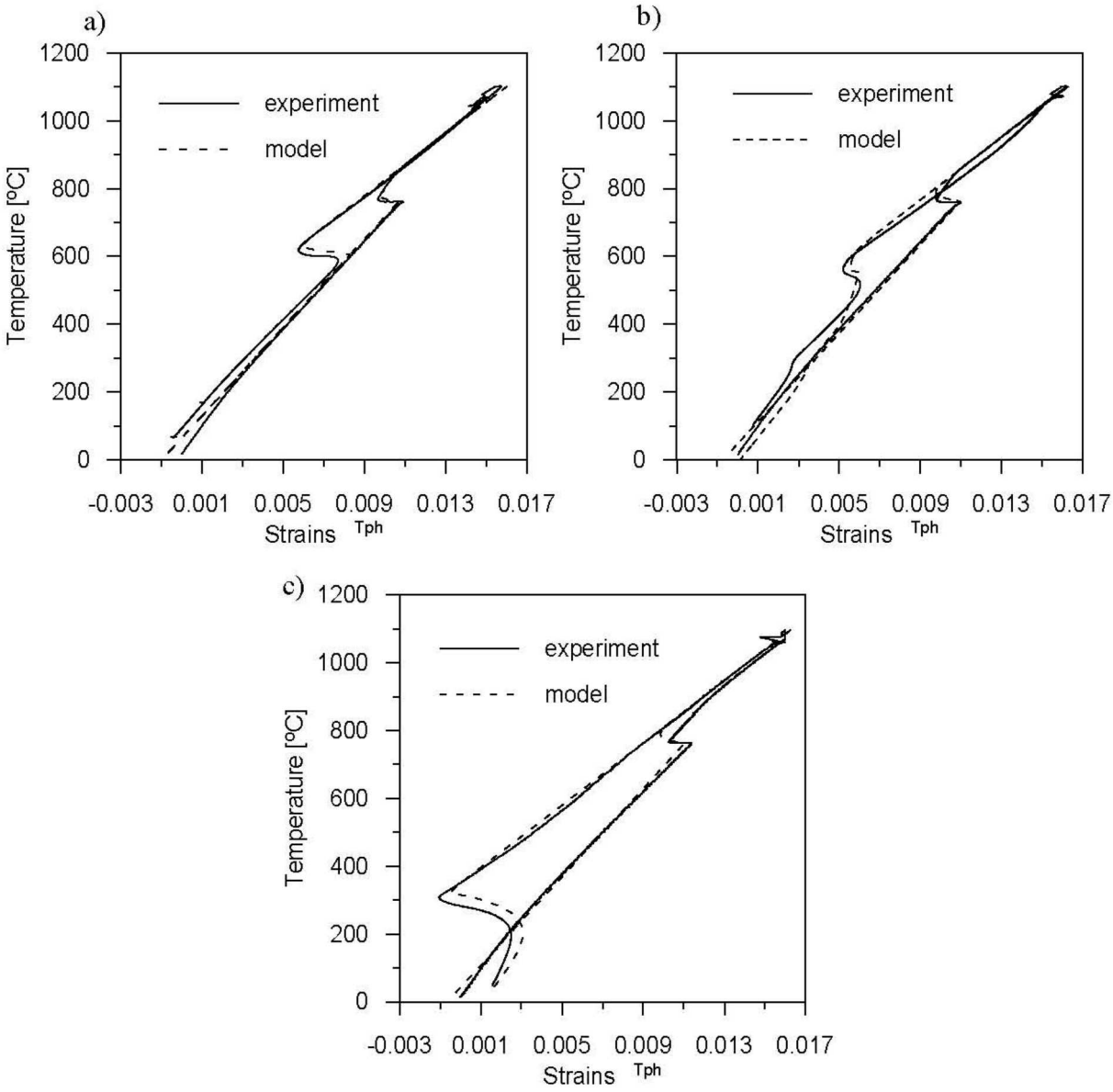

Fig. 5. The verification of the model of the phase transformations – dilatometric tests a) 10, b) 30, c) 200 [°C/s]

6. Examples of calculation

The geometry of the hardening parts surrounded by cooling liquid is presented in Fig. 6. The effect of coolant motion on distribution of bainite, martensite, thermal and structural strains was investigated. The comparative analysis of the results of calculations for the model without (example A) and with (example B) taking into account movement of coolant has been carried out. In the paper the calculation for the axisymmetric element with the notch (example C) was presented. The dimensions of the both steel elements are r=0.04 [m], h=0.06 [m], the dimensions of the notch are 0.005×0.02 [m], the radius of the container with the coolant is 0.12 [m], height is 0.12 [m]. The results of numerical solutions show the effect of the notch in the shaft on the cooling rates and fields of the kinetics of the phases. In the presented examples only natural convection is taken into account.

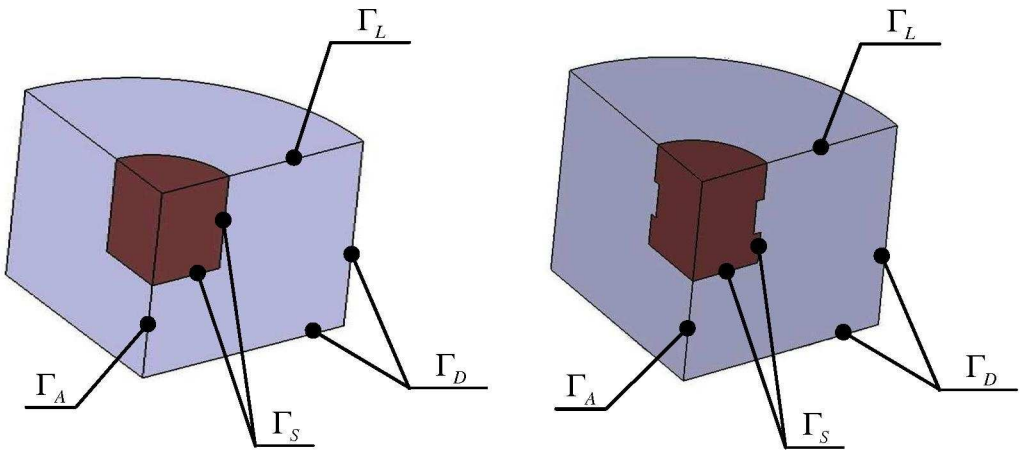

Fig. 6. Geometry of the analyzed regions for calculations a) without and with, b) with taking into account movement of coolant

Following boundary and initial conditions were introduced for the heat transport equation:

- Newton boundary condition on external boundary Γ_L with α=300 [W/m^{2}K], T_∞=300 [K],
- Neumann boundary condition on axial boundary Γ_A with q=0 [W/m^2],
- Dirichlet boundary condition on external boundary Γ_D with T_D=300 [K],
- ideal contact between hardening element and coolant on internal boundary Γ_S,
- the initial temperature of a hardening element was equal to T_H=1200 [K],
- the initial temperature of coolant T_C=300 [K].

Following boundary and initial conditions completed the Navier-Stokes equation:

- Dirichlet boundary condition on boundaries Γ_L, Γ_A, Γ_D with V_α=0 [m/s],
- initial velocities in coolant V_α=0 [m/s],
- reference temperature in coolant T_{Ref}=300 [K].

The CCT diagram for austenitization temperature was determined for 1200 [K] and was used in calculations. Material properties used in calculations are collected in Tables 1-2.

TABLE 1

The material properties of hardening elements and coolant

Material property	Hardening element	Coolant
λ [W/mK]	48.1	68
C[J/kgK]	500	1045
ρ [kg/m^3]	7760	852
μ [kg/ms]	–	2.64×10^{-4}
β [1/K]	–	2.71×10^{-4}

TABLE 2

The thermal and structural strain coefficients

Phase	α_i [1/K]	γ_i
Austenite	2.178×10^{-5}	1.986×10^{-3}
Ferrite	1.534×10^{-5}	3.055×10^{-3}
Pearlite	1.534×10^{-5}	3.055×10^{-3}
Bainite	1.171×10^{-5}	4.0×10^{-3}
Martensite	1.36×10^{-5}	6.5×10^{-3}

In the Figure 7 very large difference between fields of temperature for analyzed cases is displayed. If the convective movement of coolant is not take into account, then occurs significant decrease of the cooling rate of steel element.

The effect of notch in steel element on the field of coolant flow In the Figure 8 is presents. It shows the difficult of modelling coolant trough the boundary conditions.

The high rate of cooling occurs in the case, where the movement of coolant, favors a deeper hardening area is taking into account. This is visible on the diagrams presenting the fields bainitic and martensitic structures. (Figs 9,10,12,13). The thermal and structural strains occurring in steel element after hardening process for presented cases are shown in the Figure 11.

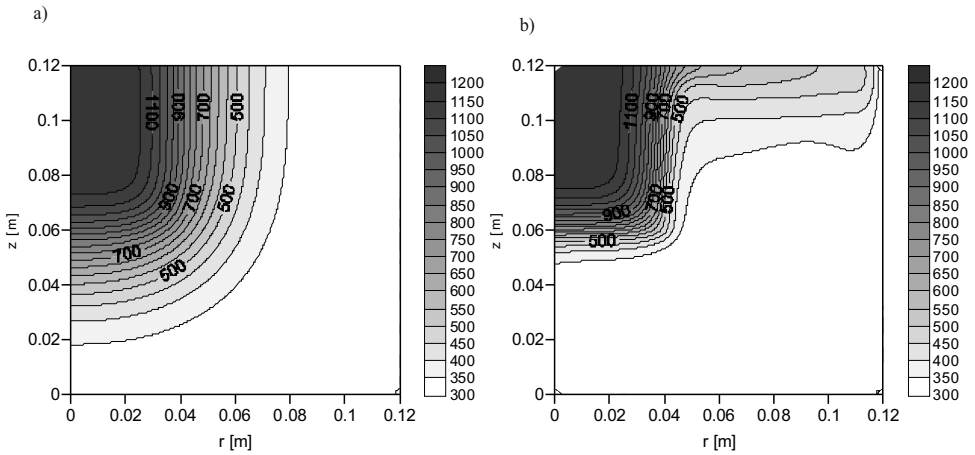

Fig. 7. Sample fields of temperature – after time t=4 [s], a) without (example A), b) with (example B) movement of coolant

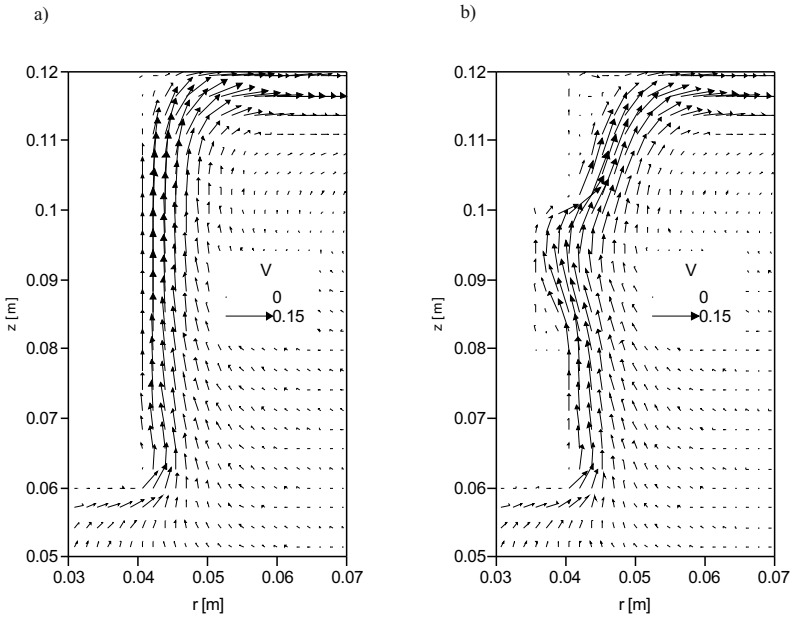

Fig. 8. Sample fields of motion vectors – after time t=4 [s], a) element without the notch (example B), b) element with the notch (example C)

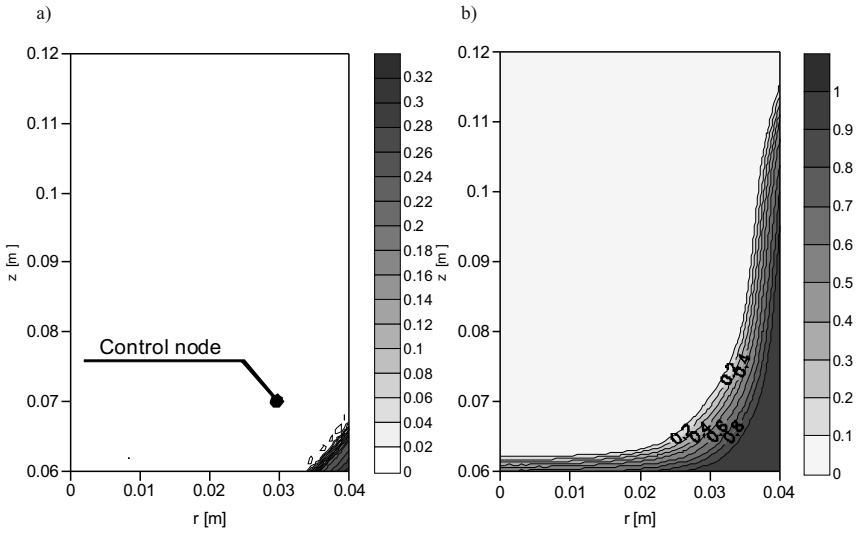

Fig. 9. The field of martensite – after cooling, a) without (example A), b) with (example B) movement of coolant

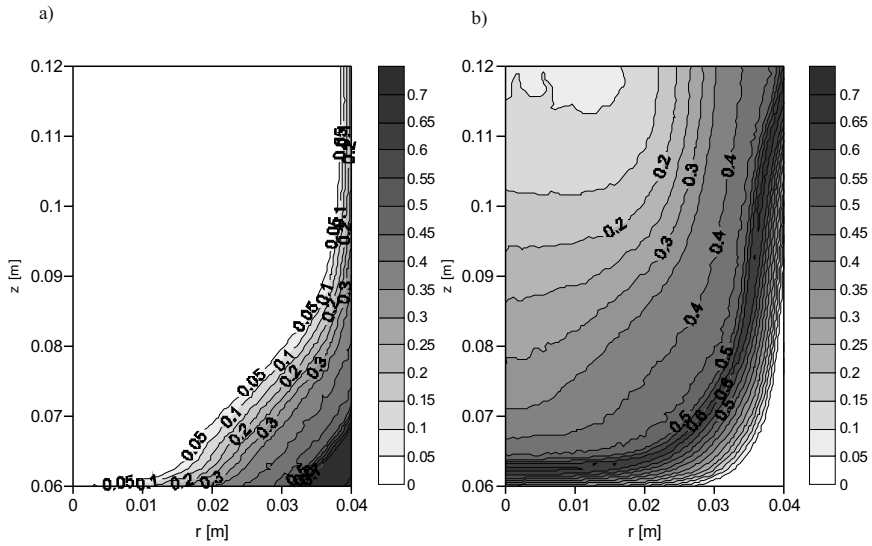

Fig. 10. The field of bainite – after cooling, a) without (example A), b) with (example B) movement of coolant

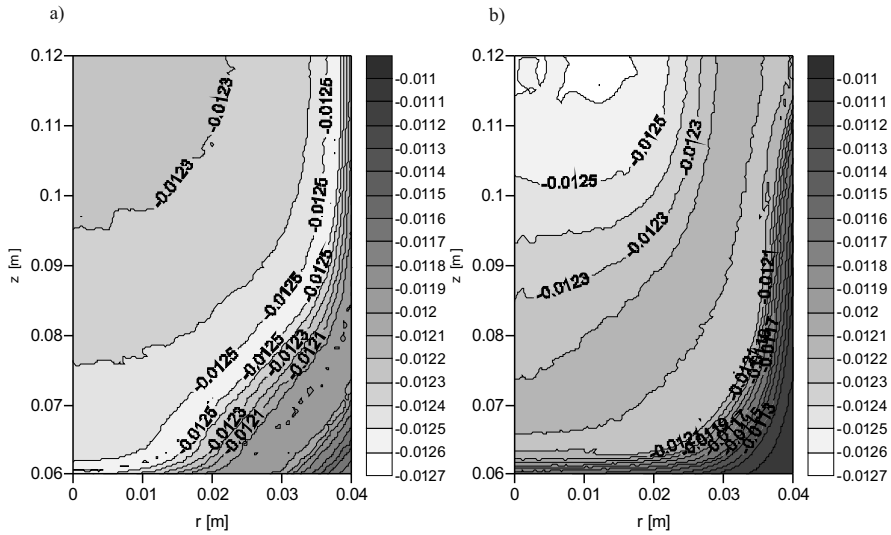

Fig. 11. The fields of thermal and structural strains – after cooling, a) without (example A), b) with (example B) movement of coolant

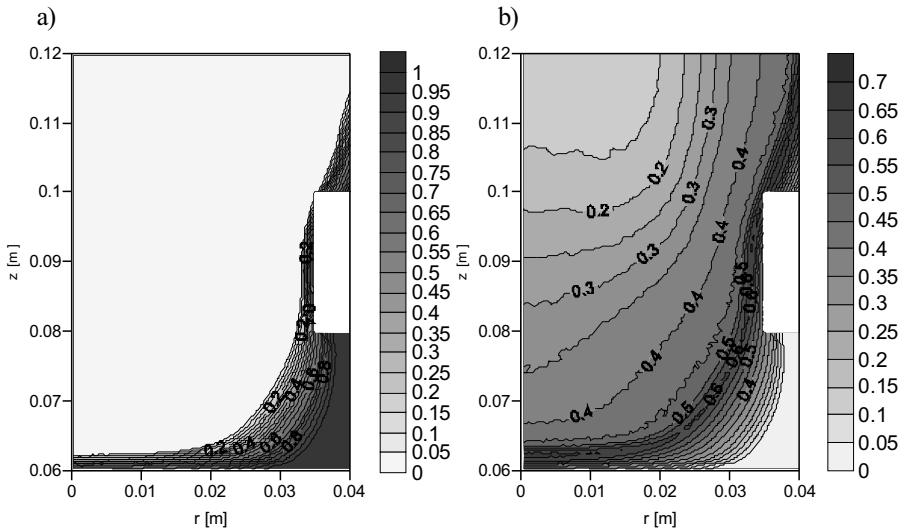

Fig. 12. The fields of phase fraction – hardening process for the shaft with the notch, a) martensite, b) bainite

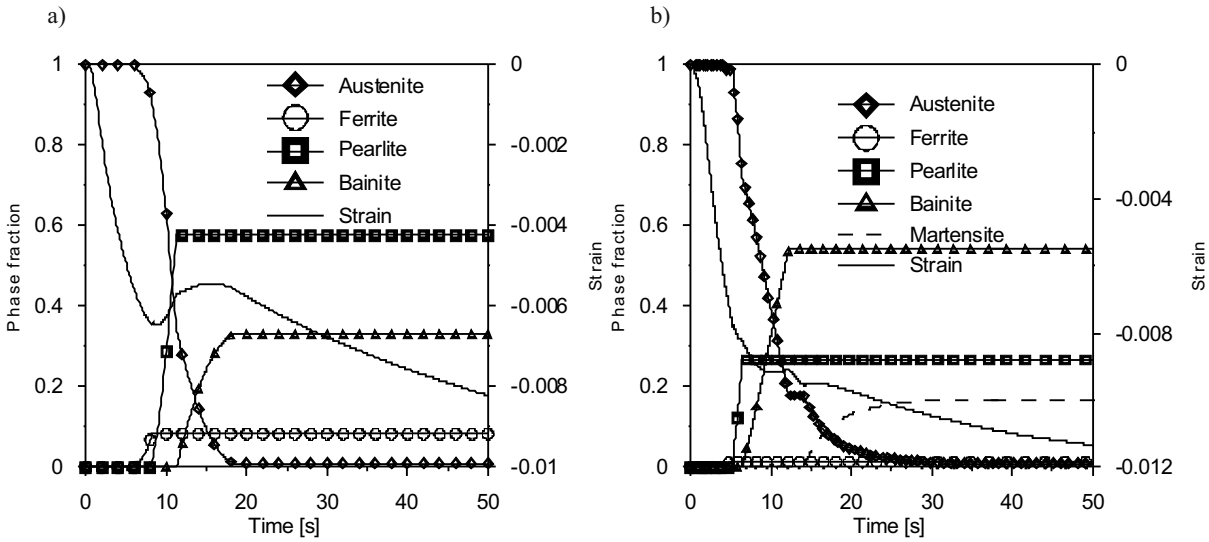

Fig. 13. The kinetics of phase in control node (see Fig. 9), a) without (example A), b) with (example B) movement of coolant

The phase transformations according to time are presented in diagrams 13. In the control nodes (see Fig. 9) the concentration of bainite is greater than 0.32 in the first variant of simulation while in the second one gives result about 0.54. The concentration of martensite in these nodes is greater than 0.16 in variant with motions of coolant. It proves significant effect of coolant motion on hardening process.

7. Conclusion

The paper presents a complex numerical model for heat treatment of steel with the movement of coolant. The solutions of the numerical model of phase transformations, temperature and coolant flow are in good conformity with the reference results (analytical solution, numerical benchmarks and experimental researches). The presented macroscopic model of phase transformation may be used to estimate of kinetics and distribution of phases in the solid state for a large number of types of steel. However, a precise CCT and CHT diagrams are required.

Comparing the solutions with and without notch in the shaft the changes in the distributions of the phase transformations due to different profile of cooling can see. In this example, it can be concluded that the predict ability of the effect of coolant on hardened element, the temperature, rate and direction of flow for geometrically complex parts is difficult without numerical modelling.

Significant differences in spatial distribution of bainite and martensite in case of considering coolant motion during hardening process in comparison with variant neglecting velocities are noticed. Cooling rates during early stage of process are definitely higher if motion of the liquid is taken into account. It results from intensive mixing of hot and cold material according to temperature gradients.

Selected numerical method can be successfully applied to problems with irregular grids. GFDM is effective in the modelling processes for complex geometries. The stabilization of this method allows one to model the flow with large values of forced coolant velocity. Without the presented stabilization, this numerical model does not lead to accurate results for the large *Peclet* numbers. This model may be used to estimate the temperature field during a cooling process for hardening steel tools. The using of complex models hardening allows the modelling of the real conditions of processes. Taking into account velocity of coolant makes it possible to determine the conditions of cooling components with complex shapes.

REFERENCES

[1] Y.J. Lan, D.Z. Li, Y.Y. Li, Modeling austenite decomposition into ferrite at different cooling rate in low-carbon steel with cellular automaton method, Acta Materialia **52**, 1721-1729 (2004).

[2] K.J. Lee, Characteristics of heat generation during transformation in carbon steels, Scripta Materialia **40**, 735-742 (1999).

[3] J. Ronda, G.J. Oliver, Consistent thermo-mechano-metallurgical model of welded steel with unified approach to derivation of phase evolution laws and transformation-induced plasticity, Comput. Methods Appl. Mech. Engrg. **189**, 361-417 (2000).

[4] A. Bokota, A. Kulawik, Model and numerical analysis of hardening process phenomena for medium-carbon steel, Archives of Metallurgy and Materials **52**, 2, 337-346 (2007).

[5] E.P. Silva, P.M.C.L. Pacheco, M.A. Savi, On the thermo-mechanical coupling in austenite–martensite phase transformation related to the quenching process, International Journal of Solids and Structures **41**, 1139-1155 (2004).

[6] J.J. Benitoa, F. Ureńaa, L. Gaveteb, Solving parabolic and hyperbolic equations by the generalized finite difference method, Journal of Computational and Applied Mathematics **209**, 208-233 (2007).

[7] T. Liszka, An interpolation method for an irregular net of nodes, Internat. J. Numer. Methods Eng. **20**, 1599-1612 (1984).

[8] R. Fletcher, Conjugate gradient methods for indefinite systems, Numerical Analysis, Lecture Notes in Mathematics **506**, 73-89 (1976).

[9] O. Axelsson, Iterative Solution Methods, Cambridge University Press, (2000).

[10] O. C. Zienkiewicz, R. Codina, A general algorithm for compressible and incompressible flow, Part I. The split characteristic based scheme, International Journal for Numerical Metods in Fluids **20**, 869-885 (1995).

[11] O.C. Zienkiewicz, R.L. Taylor, The finite element method, Butterworth-Heinemann, Fifth edition **1,2,3,** (2000).

[12] A. J. Chorin, Numerical solution of the Navier-Stokes equation, Math. Comput. **23**, 745-762 (1968).

[13] A. Kulawik, Numerical analysis of thermal and mechanical phenomena during hardening processes of the 45 steel, PhD Thesis, Częstochowa (2005), (in Polish).

[14] M. Avrami, J. Chem. Phys. **7**, 1103 (1939).

[15] H.J.M. Geijselaers, Numerical simulation of stresses due to solid state transformations. The simulation of laser hardening, Thesis University of Twente, The Netherlands, (2003).

[16] B. Chen, X.H. Peng, S.N. Nong, X.C. Liang, An incremental constitutive relationship incorporating phase transformation with the application to stress analysis, Journal of Materials Processing Technology **122**, 208-212 (2002).

[17] D. P. Koistinen, R. E. Marburger, A general equation prescribing the extent of the autenite-martensite transformation in pure iron-carbon alloys and plain carbon steels, Acta Metallica **7**, 59-60 (1959).

[18] F. Wever, A. Rose, Alas zur Wärmebehandlung von Stähle, Verlag Stahl Eisen MBH, Düsseldorf, (1954).

[19] F. Wever, A. Rose, Atlas zur Wärmebehandlung von Stähle, I Zeit Temperatur Umwandlungs Schaubilder, Verlag Stahl Eisen MBH, Düsseldorf, (1961).

[20] J. A. Cardle, A modification of the Petrov-Galerkin method for the transient convection-diffusion equation, International Journal for Numerical Methods in Engineering **38**, 171-181 (1995).

[21] U. Ghia, K. N. Ghia, C. T. Shin, High-Re Solutions for Incompressible Flow Using the Navier-Stokes Equations and a Multigrid Method, J. of Computational Physics **48**, 3, 387-411 (1982).

Received: 10 January 2011.